Available online at www.sciencedirect.com
ScienceDirect
International Journal of Multiphase Flow 34 (2008) 615–627
International Journal of Multiphase Flow
www.elsevier.com/locate/ijmulflow

The spray characteristics of a pressure-swirl injector with various exit plane tilts

Seoksu Moon [a], Essam Abo-Serie [b], Choongsik Bae [a,*]

[a] Department of Mechanical Engineering, Korea Advanced Institute of Science and Technology, 373-1, Gusong-dong, Yuseong-gu, Daejon 305-701, Republic of Korea
[b] Department of Mechanical Engineering and Design, Coventry University, Priory Street, Coventry CV1 5FB, UK

Received 3 September 2007; received in revised form 6 January 2008

Abstract

The gasoline spray characteristics of a pressure-swirl injector were investigated with various exit plane tilts. The analysis focused on the correlation between tilt angle and flow angle. Mie-scattering technique and phase Doppler anemometry were employed to analyze the macroscopic spray development and droplet size distribution of the spray. An analytical method for mass flux estimation was applied to understand the velocity distribution at the nozzle exit. The results showed that the spray shape and velocity distribution of the spray were more asymmetrical at high tilt angles. In particular, an opened hollow cone spray was formed when the tilt angle is greater than the complementary flow angle. The pressure drop inside the spray, one of the crucial factors for the swirl spray collapse at various surrounding conditions, was attenuated in this opened hollow cone spray since the pressure inside the spray was assimilated to the surrounding air pressure. The spray collapse at high fuel temperature and back pressure conditions did not appear when the tilt angle is larger than the complementary flow angle due to the reduced pressure drop inside the spray. However, tilt angle should be optimized to fulfill the requirements of spray robustness and avoid the locally rich area. The droplet size of 70° tilted nozzle spray shows a value similar to that of the original swirl spray in the plane that includes nozzle axis and the major axis of exit surface ellipse (Major axis plane) while it shows an increased value in the plane that includes nozzle axis and the minor axis of exit surface ellipse (Minor axis plane).

Keywords: Pressure-swirl spray; Tilted nozzle; Tilt angle; Flow angle

1. Introduction

Swirling injectors have been commonly used for various combustion systems such as gas turbine engines, boilers, and internal combustion engines to successfully mix fuel and oxidants with relatively low injection energy. For direct injection (DI) gasoline engines, Zhao et al. (1999) reviewed that the swirl injector has been dominantly used because of its enhanced atomization characteristics through the break-up of a conical liquid film, which is initially formed inside the nozzle. Zhao et al. (2003) also summarized the researches on DI gasoline engines and revealed that the DI gasoline engines require a well-atomized and well-stratified mixture near the spark plug. Therefore, the spray characteristics from the swirl injector should be clearly interpreted for optimal engine combustion. Previously, the wall-guided combustion system has been used as the representative combustion system of DI gasoline engines while the spray-guided combustion system is dominant technology for current DI gasoline engines. The wall-guided system forms the mixture near the spark plug using the interaction among spray, piston bowl and airflow while the spray guided system ignites the fuel around the spray envelop. The current researches on spray-guided system (Das and VanBrocklin, 2003; Honda et al., 2004; Drake et al., 2005) endeavored to clarify the required spray characteristics and mixture properties for spray-guided system. Although the swirl injector has been prevalently applied for the wall-guided combustion system of DI gasoline engines,

* Corresponding author. Tel.: +82 42 869 3044; fax: +82 42 869 5044.
E-mail address: csbae@kaist.ac.kr (C. Bae).

0301-9322/$ - see front matter © 2008 Elsevier Ltd. All rights reserved.
doi:10.1016/j.ijmultiphaseflow.2008.01.003

it caused problems in spray-guided combustion systems for DI gasoline engines due to the severe spray changes at different surrounding conditions. Therefore, for the application of a swirl injector for each combustion strategy of DI gasoline engines, the spray characteristics of the swirl injector, such as spatial velocity distribution, droplet size distribution, spray robustness and static air pressure inside the spray, should be easily controllable. There have been many researches related to the swirl spray development and atomization process. Lefebvre (1989) reviewed the researches about the swirl spray development concerning the effect of nozzle geometry and injector operating conditions, and the experimental and computational analyses (Han et al., 1997; Cousin and Nuglisch, 2001; Gavaises and Arcoumanis, 2001; Halder et al., 2002) were developed based on this review. Furthermore, lots of break-up models for liquid film have been suggested (Squire, 1953; Hagerty and Shea, 1955) and the current linear instability analyses are based on these models to clarify the atomization process of swirl spray.

Spray robustness is mainly affected by the spray momentum and static air pressure inside the spray. Generally, the spray momentum increases when the high injection pressure and smaller nozzle diameter are applied. The static air pressure inside the spray shows a smaller value compared to the atmospheric pressure as a result of the rotational motion of the air inside the spray. Although lots of researches observed the pressure drop inside the spray, most of researches (Chigier and Beer, 1964; Lucca-Negro and O'Doherty, 2001; Fu et al., 2005) concentrated this phenomenon itself. Especially for the DI gasoline engine spray, the pressure drop was not considered as a crucial factor affecting the swirl spray collapse at different injector operating conditions, but entrained air motion was considered as a main factor. However, Williams et al. (2001) briefly mentioned that the pressure difference between inner and outer parts of spray could be the reason of spray collapse. Moreover, Moon et al. (2006) measured the pressure inside the swirl spray and they argued that the pressure drop inside the swirl spray is one of the main factors related to the spray collapse.

There has been considerable research conducted on the control of the swirl spray to optimize engine combustion. Miyajima et al. (2000) and Abe et al. (2004) tested the tilted nozzle spray for the control of the swirl spray by forming a spatially non-uniform spray. Their results showed that the spray shape became asymmetrical and the spray robustness was improved when a high tilt angle was applied. However, the spatially non-uniform fuel distribution can cause a locally rich area and generate unburned combustion products, such as unburned hydrocarbon (UBHC) and particulate matter (PM). To compromise the spray robustness and non-uniform fuel distribution, the mechanism that causes the spray changes at different tilt angles should be investigated. In this study, it was judged that the correlation of flow angle and tilt angle is a crucial factor for the spray alterations at different tilt angles. Flow angle is generally determined by the swirler geometry. The large flow angle causes increased radial penetration with the improved atomization characteristics. The effect of tilt angle on the fuel flow could be correlated with the complementary flow angle, the 90° minus the flow angle, rather than the flow angle itself. When the tilt angle exceeds complementary flow angle, it is expected that the fuel does not pass some of the nozzle cut area and U or V shape spray will be formed. This shape alters the velocity distribution of spray and air pressure distribution inside the spray.

The aim of this research is to understand the spray characteristics with various exit tilt angles and determine the control mechanism of the swirl spray to fulfill the requirement of engine combustion systems. The analysis focused on the correlation between tilt angle and flow angle, which affects the spray development from the tilted nozzles. The spray characteristics are investigated with various fuel temperatures, injection pressures, and back pressures. The velocity distribution of fuel at the nozzle exit is analyzed using an analytical method for mass flux estimation. The static pressure drop inside the spray, which is one of the main factors causing the spray collapse, is also investigated at various tilt angle conditions. Moreover, the droplet size and velocity distribution of the tilted nozzle spray are analyzed and then compared with the original swirl spray.

2. Experimental setup and conditions

2.1. Macroscopic and microscopic spray analysis

To visualize the macroscopic spray development at different nozzle tilt angles, the Mie scattering method is applied as shown in Fig. 1a. The laser sheet was formed by a 6 W continuous-wave (CW) Ar-ion laser (Spectra Physics, Stabilite 2016), a cylindrical lens with a focal length of 6.5 mm, and a plano-convex lens with a focal length of 1000 mm. A CCD camera (PCO Inc., Sensicam) with a resolution of 1280×1024 pixels is utilized to capture the Mie-scattered images. The exposure time was set to 10 μs.

To measure the fuel droplet size and velocity distribution at different nozzle tilt angles, a phase Doppler anemometry (PDA) was applied, as shown in Fig. 1b. The transmitting and receiving optics of a phase Doppler anemometry (PDA) system were fixed onto a 3-dimensional traverse mechanism moving relative to the injector. The setup parameters of the PDA system are presented in Table 1. The applied velocity range was −7.5 m/s to 56 m/s. A low injection frequency at 5 Hz was applied to ensure that the time delay between two successive injections was long enough to allow all of the spray droplets to pass the location of the measurement points before the second injection started. The spray droplets at all of the measurement points were collected during 500 injections to obtain less than 10,000 droplets for each point.

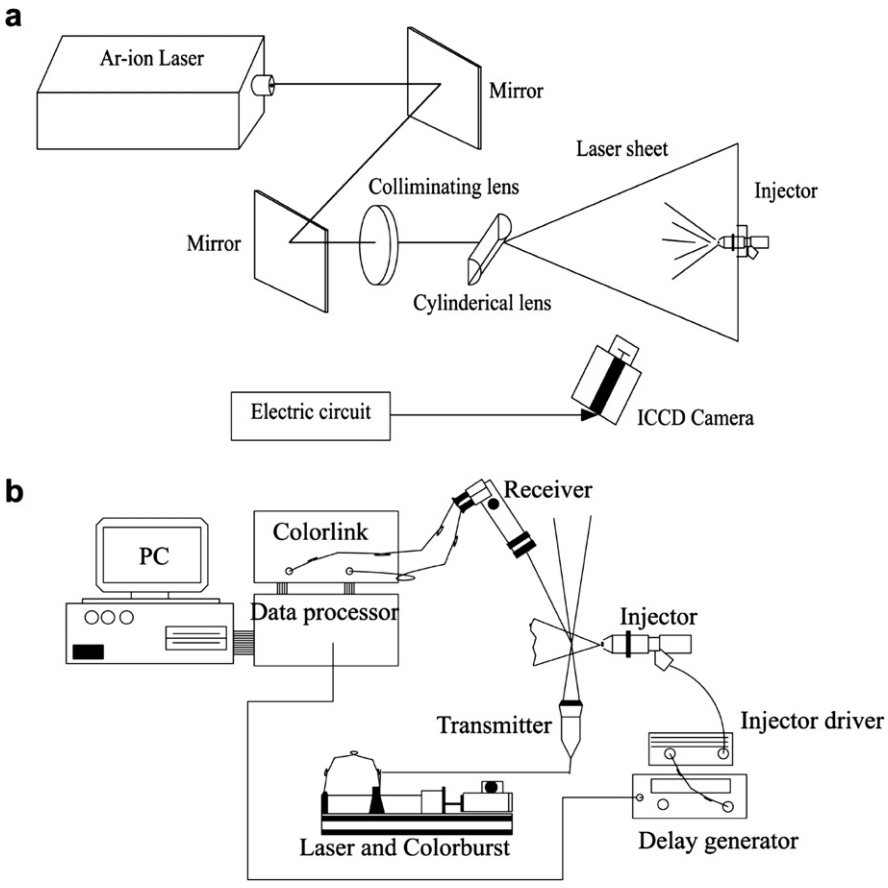

Fig. 1. Experimental setup for Mie-scattering and phase Doppler anemometry (PDA): (a) Mie-scattering and (b) phase Doppler anemometry.

Table 1
Specifications of the phase Doppler anemometry system (TSI APV)

Measurement maximum diameter	60 μm
Probe beam diameter	2.82 mm
Intersection beam angle	7.9°
Received data range	3–20 MHz
Frequency shift	5 MHz
Scattering angle	30°

2.2. Static pressure measurement inside the tilted nozzle spray

To measure the static air pressure inside the tilted nozzle spray, a pressure transducer equipped with an extended small probe, with an outer diameter of 0.6 mm and an inner diameter of 0.4 mm, was inserted into the spray center, as shown in Fig. 2. The distance from the nozzle was 0.5 mm. The pressure transducer had a response time of 1 kHz and the test range of the pressure sensor was −5 kPa to 5 kPa. The probe was aligned with the center of the nozzle hole and spray images were obtained simultaneously during the pressure measurements to make sure that the spray was not disturbed. The spray image showed that the extended probe can approach within 0.5 mm of the nozzle without disturbing the spray shape. The transducer probe orifice faced the vertical nozzle axis to measure the

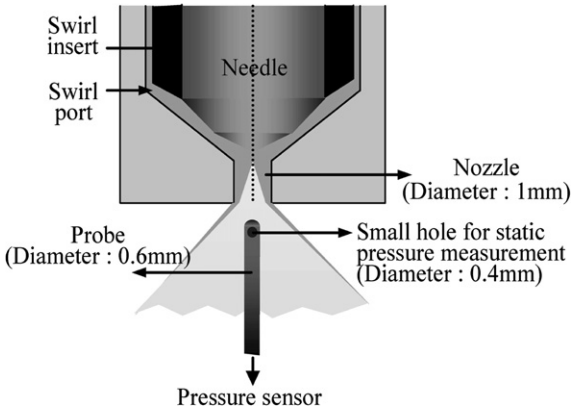

Fig. 2. Experimental setup for static pressure measurement.

static air pressure inside the spray. Because the air velocity at the centerline is very small and its direction is upward due to the central recirculation zone, the pressure measured by the probe becomes mainly a static pressure, with a negligible dynamic component.

2.3. Definition of tilt angle and complementary flow angle

The definition of tilt angle and the cross-sectional view of the applied nozzles are presented in Fig. 3. The tilt angle

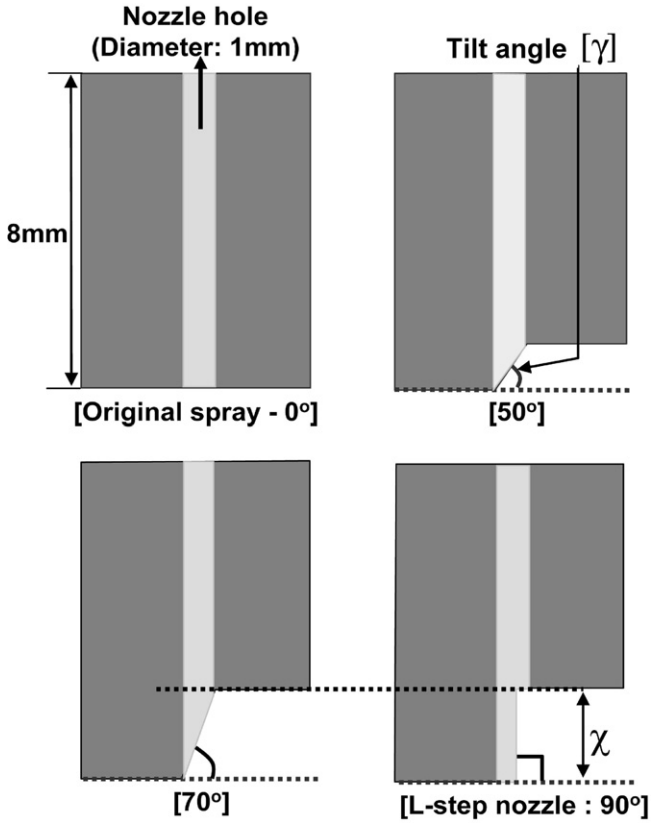

Fig. 3. Definition of tilt angle and cross-sectional view of the applied nozzles.

is defined as the angle between the bottom plane of the real nozzle and the cut plane of the tilted nozzles. The 0° tilted nozzle represents the original nozzle for the swirl spray and the 90° tilted nozzle represents the L-step nozzle. The vertical cut length (χ) of the L-step nozzle was the same as the 70° tilted nozzle. The original nozzle and tilted nozzles have the same total length of 8 mm. Fig. 4 shows the definition of flow angle (α) and complementary flow angle (δ) at the nozzle exit. A flow angle describes the ratio between the axial velocity and the tangential velocity at the nozzle exit. The flow angle is generally determined from the swirler geometry and the swirler used in this study forces the fuel to rotate with an angle of 30°. Therefore, the flow angle is considered to be 30° because previous results confirmed that the flow angle at the nozzle exit is the same as the inlet angle of the swirler.

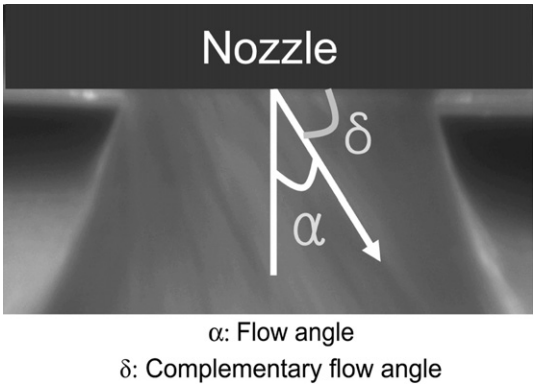

Fig. 4. Definition of flow angle and complementary flow angle.

In this study, the complementary flow angle (δ) is defined as the difference between the flow angle and 90°. It is thought that this angle is suitable for explaining the reason of spray change at different tilt angles in terms of the flow angle.

2.4. Experimental conditions

Table 2 shows the experimental conditions. The tilt angles were set to 0°, 50°, 70°, and 90°. To investigate the spray development of tilted nozzles at different surrounding conditions, different injection pressures, fuel temperatures, and ambient pressure conditions were applied. The ambient temperature condition was fixed at an atmospheric temperature and commercial gasoline was used as a test fuel.

3. Experimental results

3.1. Mass flux distribution from the tilted nozzle

Assuming constant axial and swirl velocities at the nozzle exit, it is possible to derive an equation to calculate the velocity perpendicular to the exit plane, as shown in appendix 1. The axial velocity was estimated using the continuity equation together with measuring the film thickness. The swirl velocity was measured by visualizing the trace of the droplet movement within 1 mm beneath the injector, by having a longer exposure time. The equation of volume flux distribution can be expressed by Eq. (1):

$$\mathrm{d}V = Rh(U_a \tan\alpha \sin\theta \sin\gamma + U_a \cos\gamma) \times \sqrt{\frac{\cos^2\theta}{\cos^2\gamma} + \frac{4\cos^2\theta\sin^2\theta(\cos^2\gamma-1)^2}{\cos^2\gamma(\cos^2\theta+\sin^2\theta\cos^2\gamma)} + \sin^2\theta}\,\mathrm{d}\theta \quad (1)$$

where V = volume, U_a = axial velocity, R = nozzle radius, α = flow angle, h = film thickness, γ = tilt angle and θ = angular position at the nozzle exit. Using Eq. (1), the fuel volume flux distribution can be estimated for different tilted angles as shown in Fig. 5. At one side of the nozzle the mass flow rate decreases while the other side experiences a much higher rate of fuel injection. The hollow cone spray starts to open up at one side of the nozzle when the

Table 2
Experimental conditions

Taper angle	0°, 50°, 70°, 90°
Injection pressure	5 MPa, 7 MPa
Fuel temperature	298 K, 358 K, 393 K
Ambient pressure	0.1 MPa, 0.5 MPa, 1 MPa
Ambient temperature	Atmospheric
Fuel	Commercial gasoline

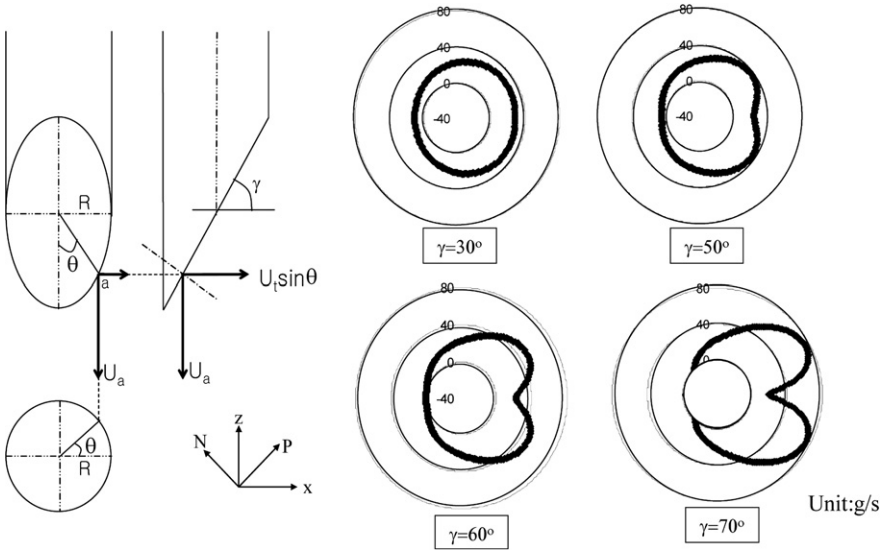

Fig. 5. The mass flux distribution at the nozzle exit for different tilt angles.

tilt angle becomes parallel to the flow direction where the fuel moves parallel to the nozzle edge without exiting the nozzle. To further explain the variation of the volume flux distribution at the nozzle exit, the calculated velocity distribution normal to the exiting plane of the nozzle is plotted for different tilt angles with a flow angle of 30°, as shown in Fig. 6. This figure shows the velocity becomes negative when the tilt angle is larger than complementary flow angle. In the negative velocity, there is no fuel mass exiting the nozzle. It also shows that increasing the tilt angle leads to a reduction in the flow velocity normal to the exiting plane. Nevertheless, the exiting area of the liquid becomes larger due to the increase in the radius and thus the arc length corresponding to one degree angle, as shown in Fig. 7.

Fig. 8 shows the side open angle at different tilt angles calculated based on the Fig. 6. The result showed that once the tilt angle reaches a value that is parallel to the flow direction in one direction of the nozzle, it opens up.

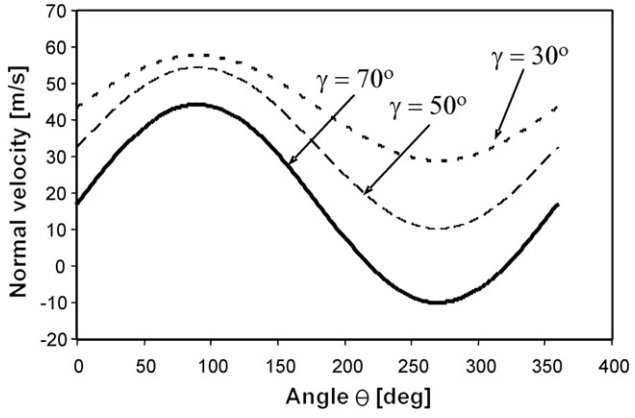

Fig. 6. The calculated velocity distribution normal to the exiting plane of the nozzle at different tilt angles (Flow angle: 30°).

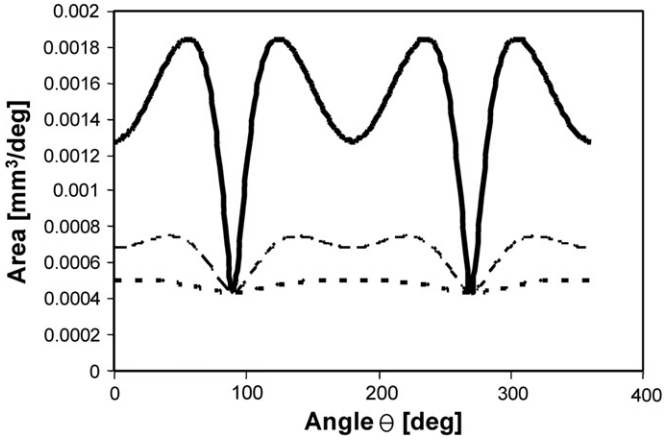

Fig. 7. The calculated exiting area distribution at different tilt angles (Flow angle: 30°).

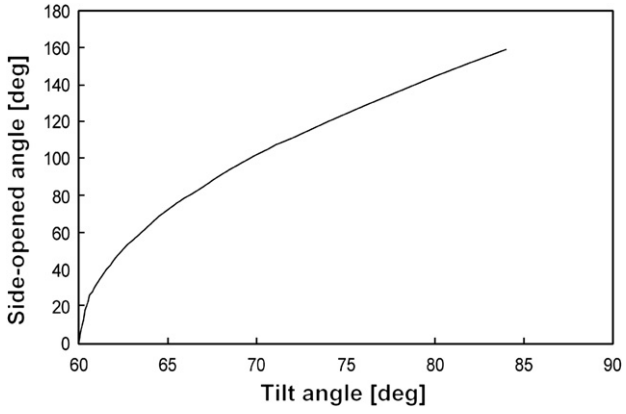

Fig. 8. The opened-side angle for different tilt angles.

3.2. Macroscopic spray development of tilted nozzles

Macroscopic spray development under various tilt angles is presented in Fig. 9. As seen in Fig. 9a, the spray

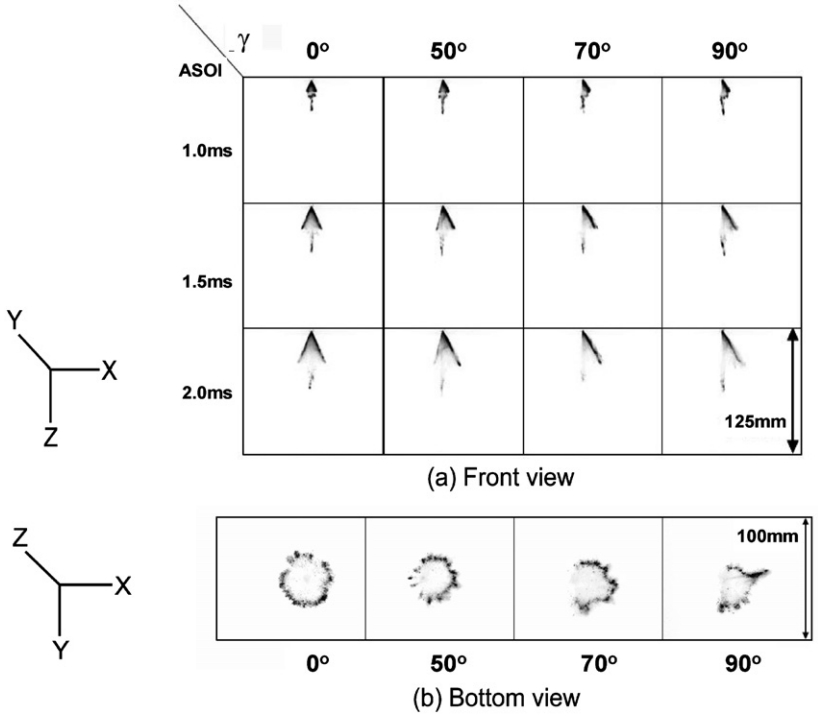

Fig. 9. Macroscopic spray images at different tilt angles: (a) front view and (b) bottom view at a plane vertically 40 mm away from the nozzle.

shape becomes asymmetrical as the tilt angle is increased, and the left side of the spray almost disappears when the tilt angle is greater than $\delta = 60°$. In particular, a U or V shape of spray is generated when the tilt angle (γ) is larger than the complementary flow angle (δ), as shown in Fig. 9b. Furthermore, the spatial fuel distribution becomes non-uniform as the tilt angle increases. Fig. 10 shows the geometric parameters for the analysis of macroscopic spray development. Two geometric parameters, main-spray penetration and spray angle, are crucial for quantifying the axial (Z) and radial (X) momentum for each spray. The main-spray penetration is defined as the vertical distance between the nozzle and the lowest location of the spray on the right side. The spray angle is defined as the angle between the nozzle axis and the line connecting the nozzle and the lowest location of the spray on the right side. Additionally, the cross diameter is defined from the bottom images, as shown in Fig. 10b. It is very useful to quantify the degree of spray collapse at different surrounding conditions. Fig. 11 shows the quantified geometric parameters under various tilt angles. The main-spray penetration shows a higher value at larger tilt angles. This means that the spray momentum is enhanced in the axial direction (Z) when a high tilt angle is applied. The spray angle has a larger value as the tilt angle is increased, and it is clear that the spray momentum is enhanced in the radial direction (X). However, the cross diameter results show the reverse trend, which means that the Y-direction spray momentum is weakened at high tilt angles. These results imply that the spatial distribution of fuel and spray momentum is becoming non-uniform as the tilt angle increases. This result can be confirmed by the mass flux estimation and velocity measurement of fuel droplets.

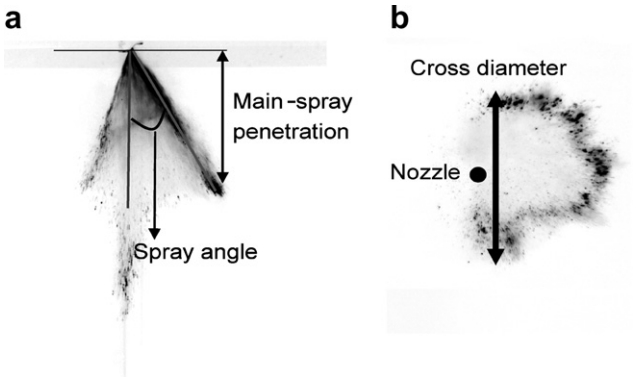

Fig. 10. Geometric parameters for spray analysis: (a) main-spray penetration and spray angle and (b) cross diameter.

3.3. Static air pressure inside the tilted nozzle spray

Fig. 12 shows the static air pressure inside the original nozzle and tilted nozzle spray. The result shows that the pressure drop inside the original swirl spray is observable. From the results of Moon (2007), it can be found that the measured value is sufficient to cause the spray collapse. However, this pressure drop is attenuated when the tilt angle is increased, as a result of the disturbed swirling motion. In particular, the attenuation of pressure drop is conspicuous when the tilt angle is more than δ. The assimilation of the air pressure between the inner and outer parts

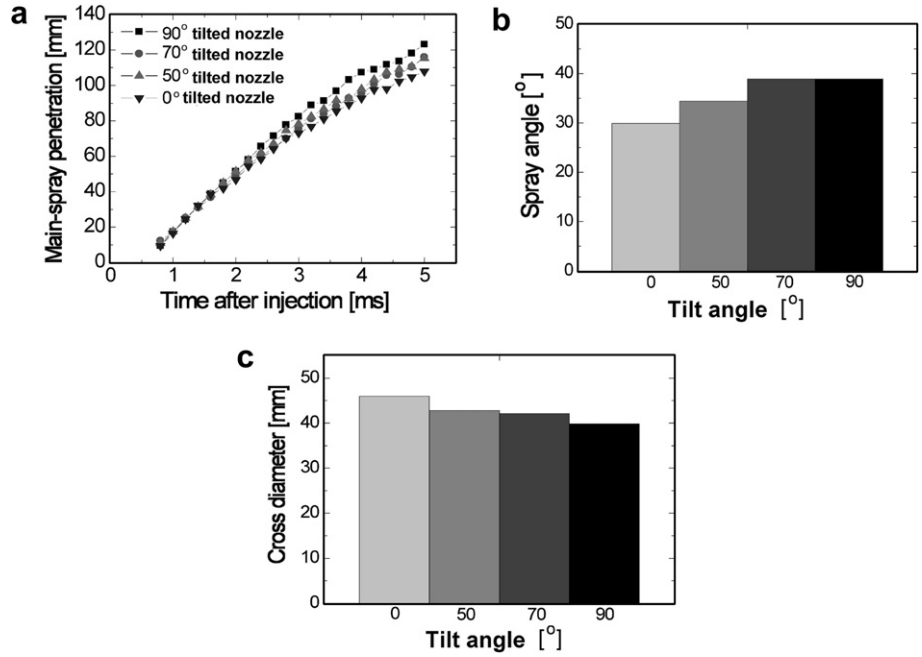

Fig. 11. Main-spray penetration, spray angle and cross diameter at different tilt angles: (a) main-spray penetration, (b) spray angle and (c) cross diameter.

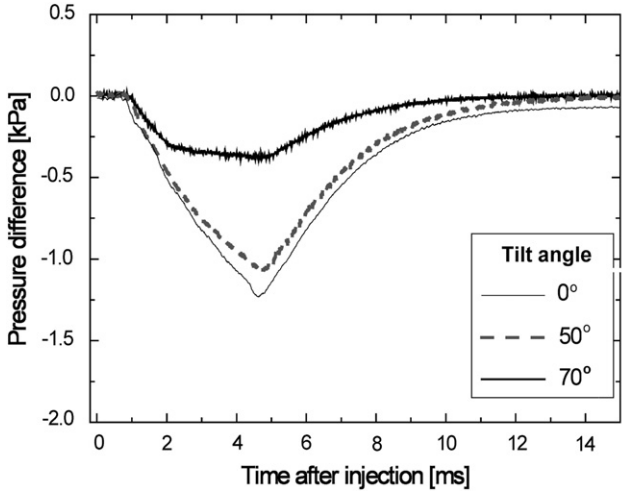

Fig. 12. Static pressure inside the tilted nozzle spray (distance from nozzle: 0.5 mm, injection pressure: 5 MPa and injection duration: 4 ms).

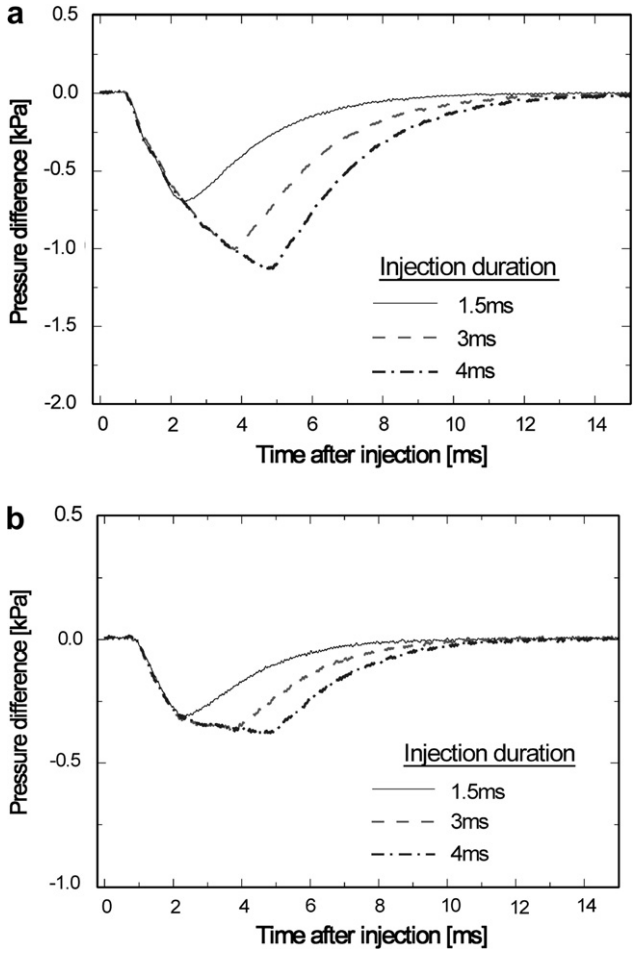

Fig. 13. Static pressure of tilted nozzles at different injection durations: (a) 50° tilted nozzle and (b) 70° tilted nozzle.

of the spray is the main reason for this phenomenon because the U or V shaped spray is formed when the tilt angle is greater than δ.

Fig. 13 shows the static pressure inside the spray from 50° and 70° tilt nozzles with variance of the injection duration. Previous research confirmed that the static pressure drop inside the spray is reinforced with the increased injection duration. In the case of a 50° tilt nozzle, the air pressure result follows the previous trend, as shown in Fig. 13a. However, there is almost no change in the static air pressure at different injection durations when the 70° tilt nozzle is applied, as shown in Fig. 13b. This means that the static air pressure inside the spray is not affected by the surrounding conditions when the tilt angle is greater than δ.

Therefore, it may be concluded that the spray will be less affected by the various surrounding conditions when the tilt angle is greater than δ.

3.4. The effect of surrounding conditions on spray development of tilted nozzles

3.4.1. The effect of fuel temperature

Zuo et al. (2000) and Chang and Lee (2005) found that the swirl spray has a smaller spray width and a longer axial penetration at high fuel temperature conditions. This is supposed to be generated from a smaller droplet size, reduced liquid film thickness, and the enhanced static pressure drop inside the spray at high fuel temperature conditions.

Fig. 14 shows the macroscopic spray development of each tilted nozzle at different fuel temperatures. Contrary to the original swirl spray, the tilted nozzle spray did not collapse at the high fuel temperature condition and the spray on the right side sustained its initial direction, as shown in Fig. 14a. Until the tilt angle reaches 70°, the spray volume gets smaller at higher tilt angles, under fuel temperatures of 358 K and 393 K. The 70° tilted nozzle spray showed the largest spray volume, while a 90° tilted nozzle (L-step) spray showed less spray volume compared to the 70° tilted nozzle spray. The quantified spray angle, main-spray penetration, and cross diameter results are plotted in Fig. 15. When the tilt angle is greater than δ, the spray angle slightly increased at high fuel temperature conditions, as shown in Fig. 15a. This phenomenon can be explained by the following discussion. Moon (2007) found that the swirl spray experiences an increased tangential velocity and sudden increase in static air pressure at the nozzle exit, when the fuel temperature is increased. This is caused by the reduced viscosity and sudden evaporation of the fuel at high fuel temperatures as explained by Zuo et al. (2000). Consequently, it makes the spray suddenly expand at the nozzle exit. However, the expanded spray abruptly collapses downstream, as a result of the reduced droplet size and enhanced static pressure drop. The reduced droplet size downstream is caused by the enhanced break-up process, and the enhanced static pressure drop is generated from the reinforced swirling motion of the swirl spray at high fuel temperatures.

This theory is also applicable to the tilted nozzle spray. The initial spray angle of the tilted nozzle spray at the noz-

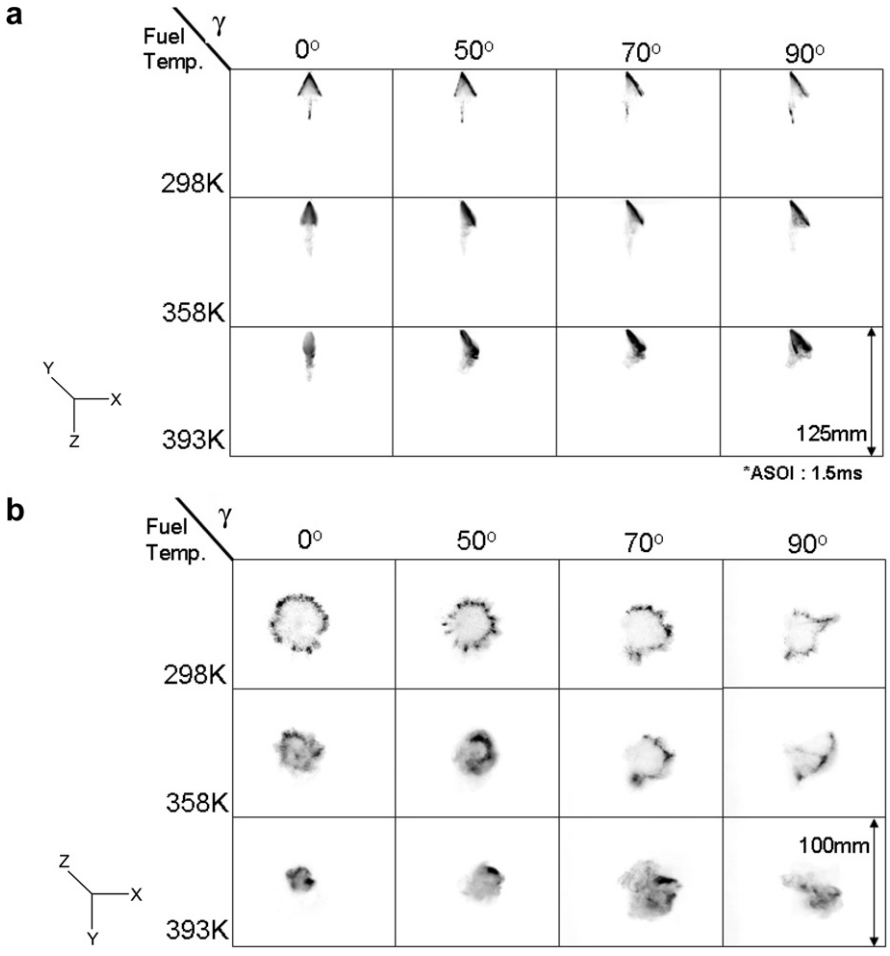

Fig. 14. Spray development of tilted nozzles under varied fuel temperatures: (a) front view and (b) bottom view at a plane vertically 40 mm away from the nozzle.

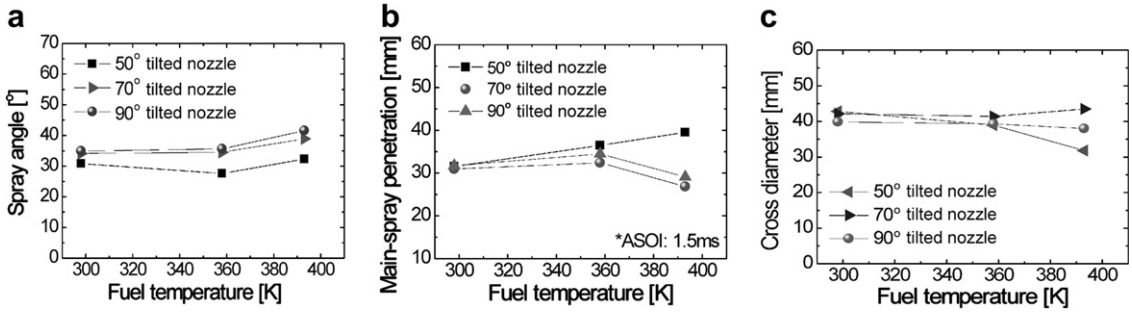

Fig. 15. Quantified geometric parameters for tilted nozzles under various fuel temperatures: (a) spray angle, (b) main-spray penetration and (c) cross diameter; ASOI: After start of injection.

zle exit increases at high fuel temperatures, as a result of increased swirling motion. However, the tilted nozzle spray does not experience enhanced static pressure drop downstream, due to disturbed swirling motion and assimilation of static pressure between the inner and outer parts of the spray. Therefore, it sustains its initial direction. That is why the increased spray angle at high temperatures is more conspicuous when the tilt angle is greater than δ.

The main-spray penetration is increased at high fuel temperature conditions when the tilt angle is less than δ, while it is reduced when the tilt angle is greater than δ, as shown in Fig. 15b. The spray does not collapse and the spray volume remains almost constant at high fuel temperatures when the tilt angle is greater than δ, as shown in Fig. 15c. In the 70° tilt nozzle, the largest spray volume is observed in the whole nozzles. This is due to the spatially uniform fuel distribution compared to the L-step nozzle. This means that there is an optimal tilt angle between 60° and 90°, which causes constant spray volume and uniform fuel distribution at high fuel temperatures. It is expected that this optimized spray will be suitable for use in an engine.

3.4.2. The effect of injection pressure and back pressure on 70° tilted nozzle spray

Fig. 16 shows the macroscopic spray images of a 70° tilted nozzle at different injection pressure and back pressure conditions. The injection pressure is set to 5 MPa and 7 MPa, and the back pressure is varied from 0.1 MPa to 1 MPa. The 70° tilted nozzle is only tested as a representative nozzle because of this nozzle's enhanced spray momentum, reduced static pressure drop inside the spray, and spatially uniform fuel distribution compared to the L-step nozzle. The results show that the spray did not collapse at high back pressure conditions, owing to the attenuated static pressure drop inside the spray and enhanced spray momentum in the X- and Z-direction. The spray penetration increased at high injection pressures, while it decreased at high back pressure conditions. The spray angle remained almost constant when the high injection pressure and back pressure conditions are applied, as shown in Fig. 17. It is clear that the 70° tilted nozzle spray is strong enough to endure high density conditions,

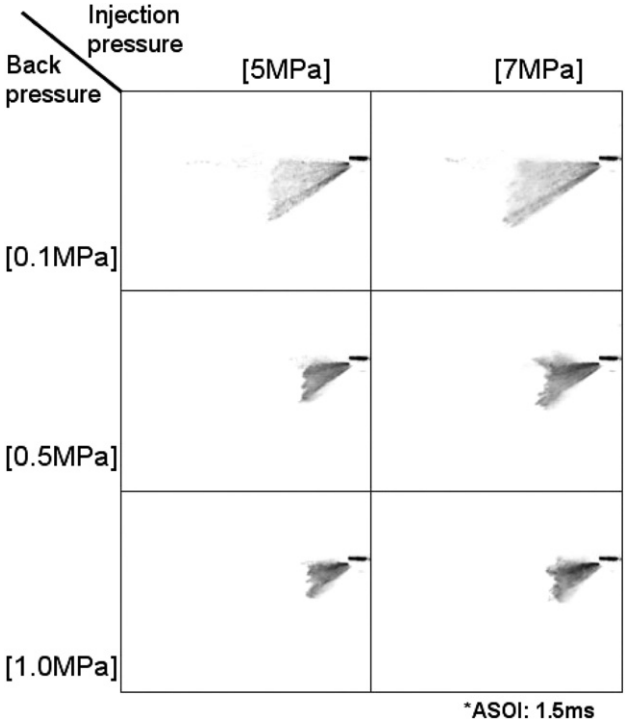

Fig. 16. Spray development of 70° tilted nozzle at different back pressure conditions.

although the applied injection pressure is relatively low compared to the multi-hole injector and outwardly open injector that are representatives of high pressure injectors for spray-guided systems. Considering that the applied nozzle length is 8 mm, the spray robustness of the 70° tilted nozzle will be enhanced if a smaller tilted nozzle length is applied.

3.5. The droplet velocity and size distribution of 70° tilted nozzle

3.5.1. Droplet velocity distribution

Fig. 18 shows the measurement points for phase Doppler anemometry (PDA). The Major axis plane represents the plane that includes nozzle axis and the major axis of exit surface ellipse while Minor axis plane represents the

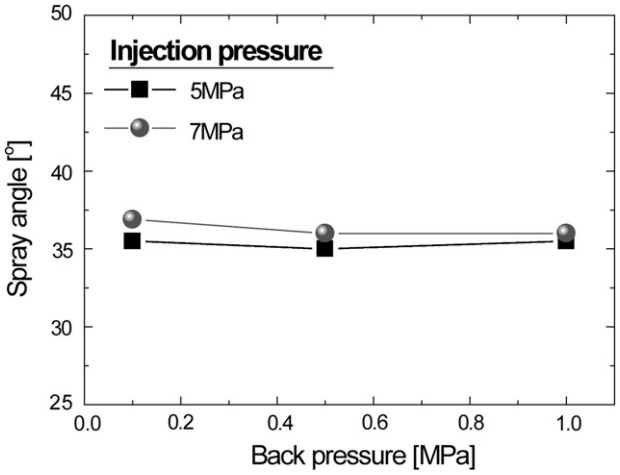

Fig. 17. Spray angle of 70° tilted nozzle at different back pressure conditions.

plane that includes nozzle axis and the minor axis of exit surface ellipse. Both measurement planes are streamwise. The measuring points of each nozzle spray were set differently because the original spray and 70° tilted nozzle spray have different spray shapes and pass different spatial locations. Due to the spatially non-uniform fuel distribution of the 70° tilted nozzle spray, the droplet size and the velocity distribution of the 70° tilted nozzle spray were measured at the Major axis and Minor axis planes, respectively. The measurement plane was vertically 40 mm away from the nozzle along the nozzle axis.

Fig. 19 shows the temporal velocity distribution of the original swirl spray and the 70° tilted nozzle spray in the Major axis plane. The maximum velocity location was chosen as the representative point for comparison of each nozzle spray. The maximum velocity location was 21 mm from the nozzle axis in the original swirl spray and was 26 mm from the nozzle axis in the 70° tilted nozzle spray. As expected from the mass flux distribution and macroscopic spray results, the velocity of the 70° tilted nozzle spray

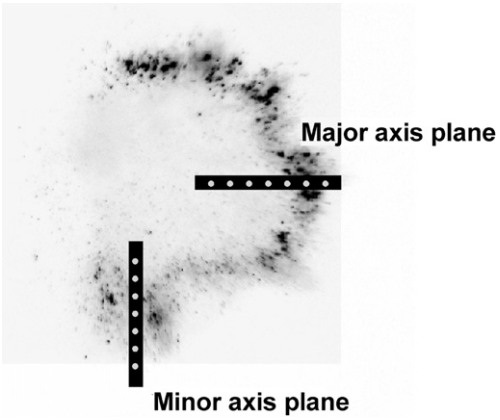

Fig. 18. Measuring points for PDA [A plane vertically 40 mm away from the nozzle along the nozzle axis, (a) original swirl spray and (b) 70° tilted nozzle spray].

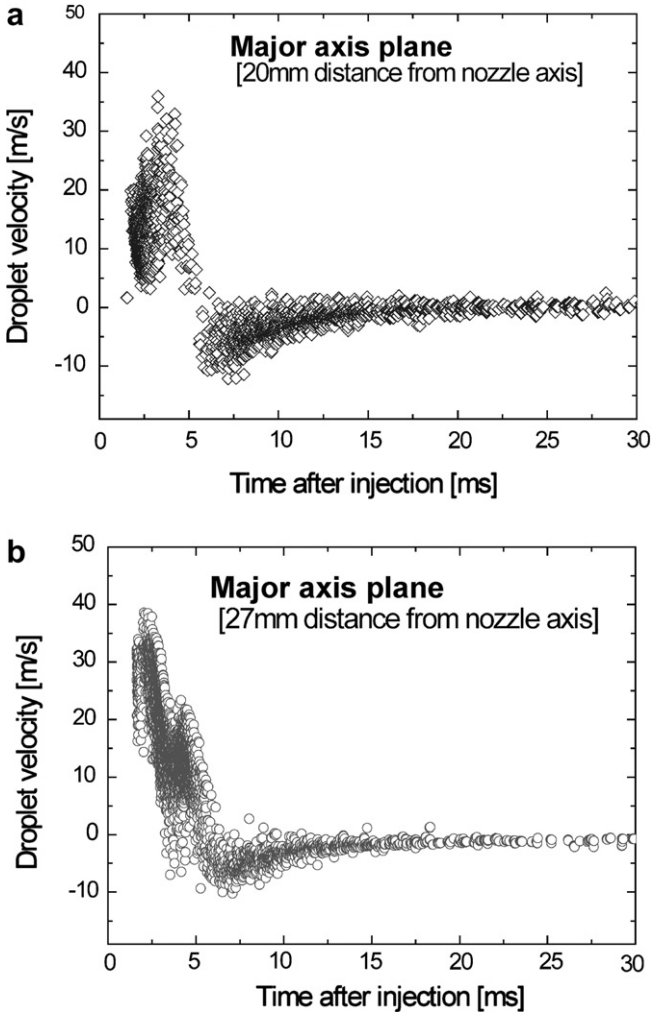

Fig. 19. Velocity distribution of original swirl spray and 70° tilted nozzle spray at Major axis plane.

showed an increased value compared to the original swirl spray at the Major axis plane. The velocity difference between the original nozzle and the 70° tilted nozzle is about 5 m/s. This result confirms that the spray momentum is reinforced in the X–Z direction by the tilted nozzle spray.

The velocity distribution of the 70° tilted nozzle in the Minor axis plane is plotted in Fig. 20. The droplet velocity at the Minor axis plane was almost half of that at the Major axis plane and it is even less than that of the original swirl spray. It demonstrates that the distribution of the droplet velocity is spatially non-uniform, although the total spray momentum is conserved.

3.5.2. Droplet size distribution

The atomization characteristics of a tilted nozzle spray are very important for the improved mixture formation near the spark plug, especially for the spray-guided combustion system. As seen from the previous results, the robust spray is formed by the 90° tilted nozzle (L-step nozzle). This type of spray is like a non-swirl injector spray, which has a strong linear momentum with little rotational

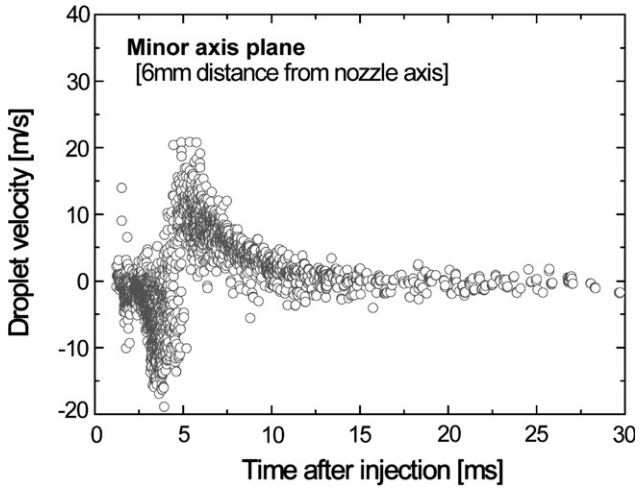

Fig. 20. Velocity distribution of 70° tilted nozzle spray at Minor axis plane.

momentum. When the rotational momentum is weakened, the spray atomization characteristic is deteriorated and the vapor phase near the liquid spray is diminished. Therefore, the spray robustness should be obtained with minimal sacrifice of the swirling motion of the spray. In this section, the atomization characteristics of the 70° tilted nozzle spray were analyzed and then compared with the original swirl spray. The 70° tilted nozzle spray is chosen as a representative tilted nozzle spray because it generates a robust spray and has better rotational momentum than the L-step nozzle.

Fig. 21 presents the droplet size profile of the original nozzle and 70° tilted nozzle sprays. The X-axis represents the radial distance from the nozzle axis. The droplet size of each location is represented by the arithmetic mean diameter (D_{10}) and Sauter mean diameter (SMD). SMD represents the volume to surface area ratio and it is a very important factor for spray and combustion analysis. The result showed that the D_{10} of the 70° tilted nozzle spray in the Major axis plane is smaller than the original swirl spray, as a result of increased injection velocity, while the SMD of the 70° tilted nozzle spray is similar to the original swirl spray as shown in Fig. 21a. This is supposedly due to the increased droplet velocity of the 70° tilted nozzle spray, although a larger portion of the fuel is located near the Major axis plane. However, the 70° tilted nozzle spray shows higher D_{10} and SMD values compared to that of the original swirl spray in the Minor axis plane. It is judged that this result is generated from a reduced droplet velocity in the Minor axis plane.

To further understand the droplet size results, the probability density functions (PDF) for the Major axis and Minor axis planes of the 70° tilted nozzle spray and original swirl spray are plotted in Fig. 22. The data obtained from all of the test points are merged and the frequency of droplet size is calculated for each nozzle. In the Major axis plane of the 70° tilted nozzle spray, the proportion of small droplets less than 20 μm has increased compared

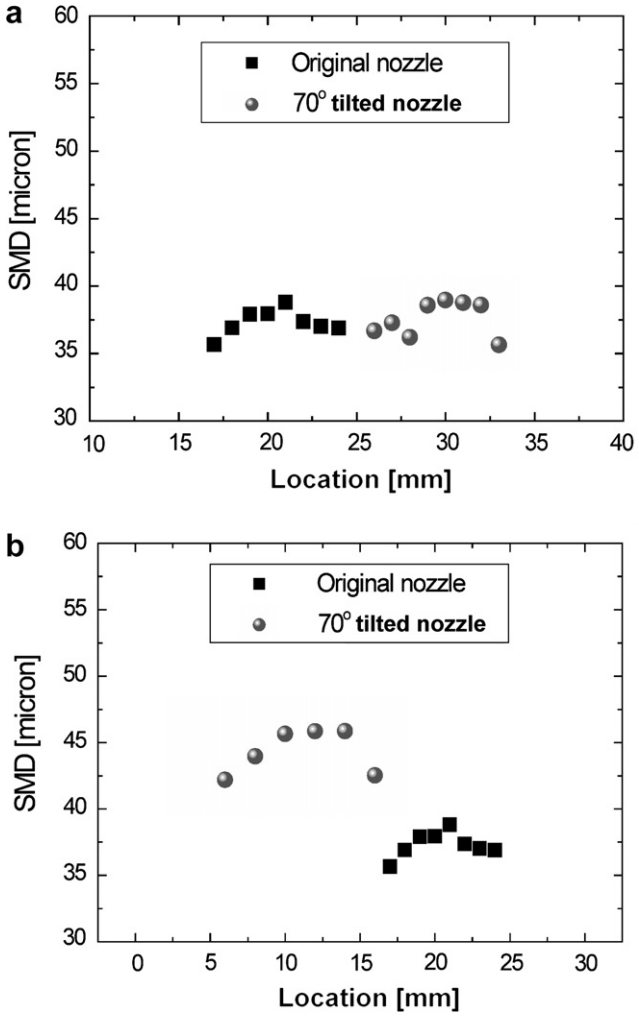

Fig. 21. Droplet size profile of 70° tilted nozzle and original swirl spray at Major axis and Minor axis planes: (a) Major axis plane and (b) Minor axis plane.

to the original swirl spray, as a result of the increased fuel velocity in the Major axis plane. However, the 70° tilted nozzle spray showed an increased proportion of large droplets whose diameter is more than 50 μm compared to the original swirl spray, owing to an increased fuel concentration. In the Minor axis plane of the 70° tilted nozzle spray, the proportion of large droplets with a diameter of more than 40 μm is significantly increased compared to the original swirl spray, due to the reduced droplet velocity.

From the above results, it was concluded that the atomization characteristics of the 70° tilted nozzle spray have slightly deteriorated compared to the original swirl spray. However, considering that the fuel is generally ignited near the main spray in spray-guided combustion, the larger portion of smaller droplets in the Major axis plane of the 70° tilted nozzle spray provide advantages for spray-guided combustion compared to the original spray. Furthermore, the 70° tilted nozzle spray does not collapse at high fuel temperature conditions; it has more advantages at normal engine operation conditions, in which the operating temperature is generally 353–393 K.

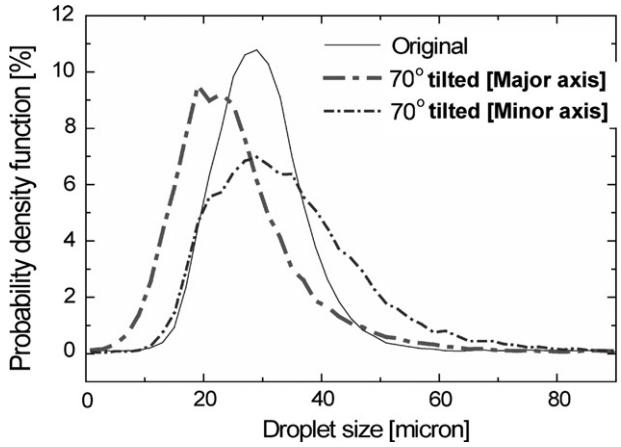

Fig. 22. Probability density function of droplet size of original nozzle and 70° tilted nozzle spray.

3.6. Speculations about the generation of robust and well-atomized swirl spray from tilted nozzle spray

It was found that the tilted nozzle spray generates robust spray when the tilt angle is greater than δ. However, the tilt angle should be optimized so that the formation of the locally rich area, which is shown in the L-step nozzle spray, is limited. The 70° tilted nozzle spray showed robust and relatively well-distributed spray compared to the L-step nozzle with a larger spray volume at high fuel temperature conditions. This larger spray volume reduces the phase gradient of the fuel and has the benefit of a well-distributed mixture formation. The droplet size of 70° tilted nozzle spray in the Major axis plane is similar to the original swirl spray and can generate even smaller droplet sizes and wider vapor distributions at high temperature conditions without severe spray collapse. Furthermore, the vapor phase area of the 70° tilted nozzle spray can be enhanced compared to the conventional sprays from non-swirl injectors because it still contains rotational momentum, although the rotational momentum is weakened compared to the original swirl spray. Therefore, it is concluded that the robust and well-atomized spray could be generated when the tilt angle is larger than δ, although the tilt angle should be optimized.

4. Conclusions

The spray and atomization characteristics of the tilted nozzles were analytically and experimentally investigated based on the correlation between the exit tilt angle and the flow angle in a pressure-swirl injector.

The opened swirl spray and attenuated pressure drop inside the spray was observed at the tilt angles of more than the complementary flow angle. The fuel distribution becomes non-uniform and the spray momentum is enhanced as the tilt angle is increased. The closed spray shape is changed to an open shape when the tilt angle is greater than the complementary flow angle, and this result is also confirmed by the mass flux distribution at the nozzle exit obtained by analytic equation. The static pressure drop inside the spray becomes attenuated as the tilt angle increases and this static pressure drop suddenly recovers to atmospheric conditions when the tilt angle is bigger than the complementary flow angle.

The tilted nozzle spray does not collapse from surrounding conditions at the tilt angles of more than the complementary flow angle. At high fuel temperatures, spray is not collapsed while slightly increased spray angle was observed when the tilt angle is more than the complementary flow angle. It was found that an optimal tilt angle exists between 60° and 90°, which leads constant spray volume and uniform fuel distribution at high fuel temperatures. The tilted nozzle spray does not collapse at high back pressure conditions when the tilt angle is greater than complementary flow angle, as a result of the enhanced spray momentum and attenuated static pressure drop inside the spray.

The 70° tilted nozzle spray shows similar atomization characteristics with original swirl spray. At the Major axis plane that includes nozzle axis and the major axis of exit surface ellipse, the droplet velocity of the tilted nozzle is greater than that of the original swirl spray while it gets slower at the Minor axis plane that includes nozzle axis and the minor axis of exit surface ellipse. The SMD of the 70° tilted nozzle spray is similar to that of the original swirl spray at the Major axis plane. However, it shows a deteriorated atomization characteristics at the Minor axis plane compared to the original swirl spray. These results originate from the spatially non-uniform velocity distribution. The tilted nozzle spray shows the possibility of generating robust, well-atomized and spatially uniform spray with increase in vapor phase near the main spray.

Acknowledgement

The authors would like to thank for the financial support of the Combustion Engineering Research Center (CERC) and Future Vehicle Technology project in Korea.

Appendix. Analysis of the fuel flow flux along the circumference of tilted nozzle

Assume the axial and tangential velocities at the nozzle exit are constant:

$$U_a = -U_z, \quad \text{and } U_t = U_a \tan\alpha$$

where α is the flow angle that has been measured from the images.

To calculate the mass flow rate at different locations, the velocity perpendicular to the nozzle exit plane has to be calculated for different angles, θ, in the N-direction, as shown in the figure.

The axial and tangential velocity can be calculated in x–z coordinates as follows:

$$U_x = U_t \sin\theta \quad \text{and } U_z = -U_a$$

The velocity components in the N–P coordinate that is rotated by an angle, which is equal to the tilt angle is:

$$U_P = U_x \cos\gamma + U_z \sin\gamma = U_t \sin\theta\cos\gamma - U_a \sin\gamma$$

and

$$U_N = -U_x \sin\gamma + U_z \cos\gamma = -U_t \sin\theta \sin\gamma - U_a \cos\gamma$$

The volume flow rate through an angle $d\theta$ can be calculated as follows:

$$dV = U_N h\, ds$$

where h is the film thickness and ds is the arc length.

An approximate calculation to the arc length ds corresponding to an angle $d\theta$ could be deduced from the following equation:

$$ds = \sqrt{R_2^2 + \left(\frac{dR_2}{d\theta}\right)^2}\, d\theta$$

where R_2 is the radius of the ellipse at any angle θ which could be calculated from the geometry from the following equation:

$$R_2^2 = \frac{R^2\cos^2\theta}{\cos^2\gamma} + R^2\sin^2\theta$$

Therefore,

$$ds = R\sqrt{\frac{\cos^2\theta}{\cos^2\gamma} + \frac{4\cos^2\theta\sin^2\theta(\cos^2\gamma-1)^2}{\cos^2\gamma(\cos^2\theta+\sin^2\theta\cos^2\gamma)} + \sin^2\theta}\, d\theta$$

The volume and mass of injected fuel at an angle θ within a step of $d\theta$ becomes:

$$dV = Rh(U_a\tan\alpha\sin\theta\sin\gamma + U_a\cos\gamma) \times \sqrt{\frac{\cos^2\theta}{\cos^2\gamma} + \frac{4\cos^2\theta\sin^2\theta(\cos^2\gamma-1)^2}{\cos^2\gamma(\cos^2\theta+\sin^2\theta\cos^2\gamma)} + \sin^2\theta}\, d\theta$$

$$dm = \rho Rh(U_a\tan\alpha\sin\theta\sin\gamma + U_a\cos\gamma) \times \sqrt{\frac{\cos^2\theta}{\cos^2\gamma} + \frac{4\cos^2\theta\sin^2\theta(\cos^2\gamma-1)^2}{\cos^2\gamma(\cos^2\theta+\sin^2\theta\cos^2\gamma)} + \sin^2\theta}\, d\theta$$

The above equation estimates the volume and mass distribution of the liquid injected from the nozzle with angle for different nozzle tilt angle, flow angle, and axial velocity.

The side-opened angle could be deduced by assuming the mass flow rate is equal to zero. Solving this equation will lead to an equation as below which identify the angle at which the mass flow rate reaches to zero.

$$\sin\theta = \frac{-1}{\tan\alpha\tan\gamma} \quad \text{where } \gamma \geqslant (90-\alpha)$$

Accordingly, the relationship between the flow angle and tilt angle for different open side angles can be established.

Side-opened angle $= 2(90-\theta)$

This equation is only valid for the tilt angles larger than the complementary flow angle.

References

Abe, M., Okamoto, Y., Kadomukai, Y., 2004. Fuel spray pattern control using L-step nozzle for swirl-type injector. SAE Trans. 1832, 233–238.

Chang, D., Lee, C.F., 2005. Development of a simplified bubble growth model for flash boiling sprays in direct injection spark ignition engines. Proc. Combust. Inst. 30, 2737–2744.

Chigier, N.A., Beer, J.M., 1964. Velocity and static pressure distributions in swirling air jets issuing from annular and divergent nozzles. J. Basic Eng. D 86, 788–796.

Cousin, J., Nuglisch, H.J., 2001. Modeling of internal flow in high pressure swirl injectors. SAE Trans. 110, 806–814.

Das, S., VanBrocklin, P.G., 2003. Effect of design and operating parameters on the spray characteristics of an outward opening injector. In: Thirteenth International Multidimensional Engine Modeling User's Group Meeting, Detroit, USA.

Drake, M.C., Fansler, T.D., Lippert, A.M., 2005. Stratified-charge combustion: modeling and imaging of a spray-guided direct-injection spark-ignition engine. Proc. Combust. Inst. 30, 2683–2691.

Fu, Y., Jong, S.M., Tacina, R., 2005. Characteristics of the swirling flow generated by an axial swirler. In: Proceedings of ASME Turbo Expo 2005, Reno-Tahoe, USA.

Hagerty, W.W., Shea, J.F., 1955. A study of the stability of plane fluid sheets. J. Appl. Mech. 22, 509–514.

Gavaises, M., Arcoumanis, C., 2001. Modelling of sprays from high-pressure swirl atomizers. Int. J. Engine Res. 12, 95–117.

Halder, M.R., Dash, S.K., Som, S.K., 2002. Initiation of air core in a simplex nozzle and the effects of operation and geometrical parameters on its shape and size. Exp. Therm. Fluid Sci. 26, 871–878.

Han, Z., Fan, L., Reitz, R.D., 1997. Multidimensional modeling of spray atomization and air-fuel mixing in a direct-injection spark-ignition engine. SAE Trans. 106, 1423–1441.

Honda, T., Kawamoto, M., Katashiba, H., Sumida, M., Fukutomi, N., Kawajiri, K., 2004. A study of mixture formation and combustion for spray guided DISI. SAE Trans. 1832, 189–196.

Lefebvre, A.H., 1989. Atomization and Sprays. Hemisphere Publishing Corporation.

Lucca-Negro, O., O'Doherty, T., 2001. Vortex breakdown: a review. Prog. Energy Combust. Sci. 27, 431–481.

Miyajima, A., Okamoto, Y., Kadomukai, Y., Togashi, S., Kashiwaya, M., 2000. A study on fuel spray pattern control of fuel injector of gasoline direct injection engines. SAE Trans. 109, 1242–1251.

Moon, S., 2007. The spray and combustion characteristics from swirl and slit injectors for direct-injection spark-ignition engines. Ph.D. thesis, Korea Advanced Institute of Science and Technology.

Moon, S., Abo-Serie, E., Shin, H., Bae, C., 2006. Static pressure distribution inside the swirl spray. In: 10th International Conference on Liquid Atomization and Spray Systems (ICLASS), Kyoto, Japan.

Squire, H.B., 1953. Investigation of the instability of a moving liquid film. Brit. J. Appl. Phys. 4, 167–169.

Williams, P.A., O'Donoghue, S., Anderson, R.W., Richardson, S.H., 2001. An experimental study of the spray characteristics of pressure-swirl atomizers for DISI combustion systems. SAE Trans. 110, 1259–1280.

Zhao, F., Lai, M.C., Harrington, D.L., 1999. Automotive spark-ignited direct-injection gasoline engines. Prog. Energy Combust. Sci. 25, 4–8.

Zhao, F., Harrington, D.L., Lai, M., 2003. Automotive Gasoline Direct-Injection Engines. Society of Automotive Engineers.

Zuo, B., Gomes, A.M., Rutland, C.J., 2000. Modeling superheated fuel sprays and vaporization. Int. J. Engine Res. 1, 321–336.